

Imaging Protoplanetary Disks with a Square Kilometer Array

D.J. Wilner^a

^a Harvard-Smithsonian Center for Astrophysics, 60 Garden St., Cambridge, MA, 02138 USA

The recent detections of extrasolar giant planets has revealed a surprising diversity of planetary system architectures, with many very unlike our Solar System. Understanding the origin of this diversity requires multi-wavelength studies of the structure and evolution of the protoplanetary disks that surround young stars. Radio astronomy and the Square Kilometer Array will play a unique role in these studies by imaging thermal dust emission in a representative sample of protoplanetary disks at unprecedented sub-AU scales in the innermost regions, including the “habitable zone” that lies within a few AU of the central stars. Radio observations will probe the evolution of dust grains up to centimeter-sized “pebbles”, the critical first step in assembling giant planet cores and terrestrial planets, through the wavelength dependence of dust emissivity, which provides a diagnostic of particle size. High resolution images of dust emission will show directly mass concentrations and features in disk surface density related to planet building, in particular the radial gaps opened by tidal interactions between planets and disks, and spiral waves driven by embedded protoplanets. Moreover, because orbital timescales are short in the inner disk, synoptic studies over months and years will show proper motions and allow for the tracking of secular changes in disk structure. SKA imaging of protoplanetary disks will reach into the realm of rocky planets for the first time, and they will help clarify the effects of the formation of giant planets on their terrestrial counterparts.

1. Introduction

The detection of extrasolar planets has fired the imagination of modern society to the possibility of finding other Earth-like planets. The search for terrestrial exoplanets that could harbor life is one of the most publicly enthralling and scientifically and philosophically important ventures of the 21st century. The Square Kilometer Array (SKA) will make a fundamental and crucial contribution to this effort as the only observational facility currently planned that will be capable of imaging the birth sites of terrestrial planets in the dusty disks surrounding newly formed stars—the “cradle of life”.

The dusty disks that naturally arise from the star formation process are the sites where planets are made[1]. Gravitational, hydrodynamic, magnetic, and chemical processes are all active in determining the evolution of disks and their planet forming activity. The inner disk, within a few AU of the central star, is the “habitable zone” for stars like the Sun, within which terrestrial planets or the moons of gas giants are most likely to have environments favourable for the development of

life. The SKA will have the unique capability to image thermal dust emission at unprecedented sub-AU scales within this zone. The surprising discovery of giant exoplanets located well within the habitable zone raises many questions: What accounts for the diversity in planetary systems? Are terrestrial planets common in the habitable zone? Do giant planets form in the inner disk or do they migrate there, and what are the implications for terrestrial planets? Is our Solar System an exceptional case? The answers to these questions will come from a better understanding of the structure and evolution of protoplanetary disks.

2. Protoplanetary Disks

2.1. Observational Challenges

By the time stars of $\sim 1 M_{\odot}$ reach ages of ~ 1 Myr, the majority of their natal circumstellar envelope material has been dispersed and they are revealed at optical wavelengths as T-Tauri stars. At this stage, the accretion disks surrounding the stars where planets form become readily accessible to observation at many wavelengths. These observations face several significant challenges:

- The bulk of the disk mass is comprised of molecular hydrogen that does not emit at the low temperatures characteristic of the material. The disk can be studied only through its minor constituents, in particular (1) dust grains, through thermal emission and scattered starlight, and (2) trace molecules with fractional abundances of 10^{-4} or less, many of which are frozen out onto dust grains except in the heated upper layers of disk atmospheres where they participate in a complex chemistry.
- The angular scales of even nearby disks are small. For the large sample of ~ 1 Myr old stars associated with the nearest dark clouds like Taurus, Ophiucus and Chamaeleon at ~ 150 pc, the 10 and 2 AU diameters of the orbits of Jupiter and Earth subtend only 65 and 13 milliarcseconds respectively. Thus very high angular resolution is required to discern disk structures at the size scales of interest.
- The inner disk, especially within a few AU of the central star, is difficult to probe at most wavelengths even when sufficient angular resolution may be obtained. In the optical, the high contrast of scattered light from the disk with the stellar photosphere is problematic, and very careful point-spread-function subtraction or coronography is essential. Even with these techniques, the habitable zone remains inaccessible. At millimeter wavelengths, dust emission remains optically thick at the typical column densities of 100 g cm^{-2} or more, and observations cannot penetrate into the disk to reveal structure.

2.2. The Role of the SKA

Though the investigation of protoplanetary disk environments has not been a traditional topic for radio astronomy, the SKA will uniquely meet the challenges of imaging the inner regions of protoplanetary disks. Significant collecting area on ~ 1000 km scales operating at wavelengths ~ 22 GHz (~ 1.3 cm) will provide sufficient sensitivity for imaging thermal dust emission at

\sim milliarcsecond resolution. The short centimeter wavelengths accessible to the SKA are particularly advantageous at this high angular resolution since the dust emission remains optically thin and samples the high surface density regions of the inner disks that remain opaque at millimeter wavelengths. Also, emission from circumstellar dust dominates emission from the stellar photosphere, generally by many orders of magnitude at these wavelengths, and there is no contrast problem between disk and star.

SKA images of inner disks will have angular resolution an order of magnitude higher than for any other planned observational facility, including the Thirty Metre Telescope at optical wavelengths, the James Webb Space Telescope in the infrared, and the Atacama Large Millimeter Array. This order of magnitude in resolution is an especially significant one, as it enables imaging of structure in the habitable zone of nearby protoplanetary disks for the first time.

2.3. Global Properties

Since most of the disk material surrounding low mass stars beyond a few stellar radii is at low temperatures, well below 1000 K, dust provides the dominant source of continuous opacity. Though a large fraction of the disk energy is radiated in the far-infrared, a spectral range difficult to access from the ground and lacking large apertures in space, a lot has been learnt about the global properties of protoplanetary disks from analyses of their overall spectral energy distributions, which are sensitive to the size, shape, and mass of the disk. Figure 1 shows the spectral energy distribution of TW Hya, a nearby T-Tauri star of spectral type K7, from optical to radio wavelengths, together with a model of disk emission.

The shape of the spectral energy distribution of TW Hya is fit very well by the disk model. The spectral energy distributions of most T-Tauri stars are generally explained very well by disk models with a parameterized dust absorption coefficient of power law form $\kappa_\nu = \kappa_d(\nu/10^{12} \text{ Hz})^\beta$, with $\beta \sim 1$ and normalization $\kappa_d = 0.1 \text{ cm}^2 \text{ g}^{-1}$ (see [4]). This expression hides many uncertainties associated with grain sizes, composition, and

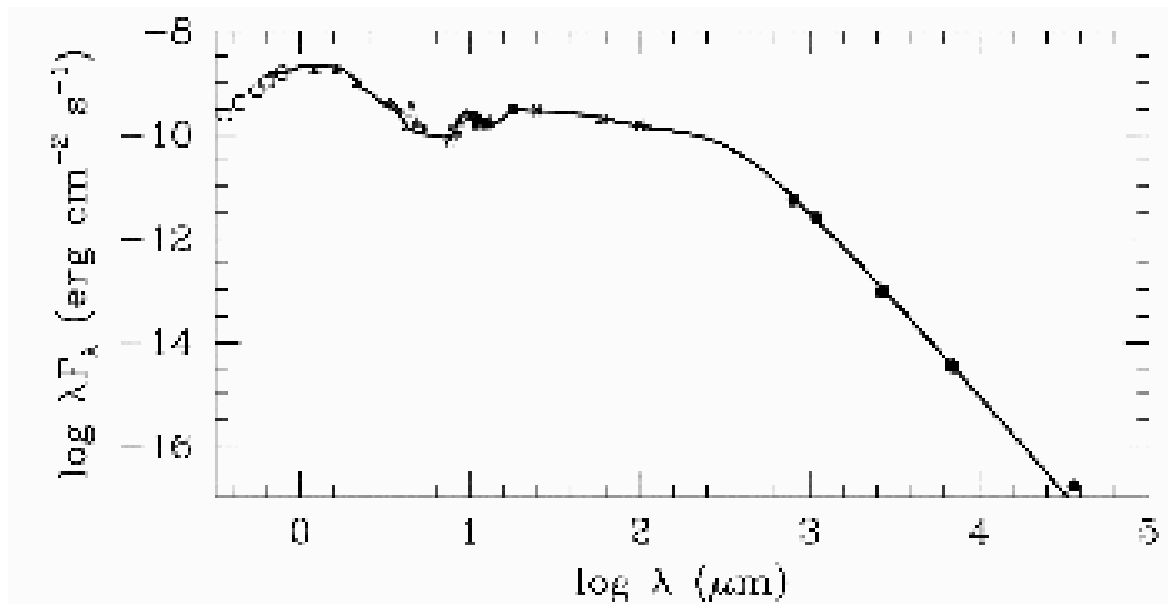


Figure 1. The spectral energy distribution of the nearby young star TW Hya (from [2]). At optical wavelengths, the stellar photosphere dominates. At mid-infrared and longer wavelengths, the broad continuous emission comes from dust particles in a circumstellar disk heated primarily by starlight impinging on the disk surface. The panchromatic nature of the emission is due to the broad range of temperatures in the disk, which has radial and vertical gradients.

also the dust-to-gas ratio, e.g. the emissivity must be affected by the evaporation of different grain constituents, starting with water ices at $T \sim 200$ K. Nonetheless, this expression is commonly adopted and provides a useful first-order description.

The dust emission from a typical protoplanetary disk starts to become optically thin at wavelengths longward of a few hundred microns, which becomes readily accessible to observation through atmospheric windows at millimeter and radio wavelengths. In this regime, where all but the inner disk regions are optically thin, the observed emission is directly proportional to disk mass, weighted by temperature. Early analyses of spectral energy distributions of T-Tauri stars like TW Hya provided strong support for disk geometries, suggesting minimum outer radii of 10's to 100's of AU [3] and masses of gas + dust from 0.001 to 0.1 M_{\odot} , sufficient to form planetary systems like our own [4]. The reasons for the wide range in protoplanetary disk properties is not known, but it is likely that initial conditions, such as the angular momentum content of the parent molecular core, as well as environmental effects, are important.

Statistical studies of large samples suggest that disks dissipate on timescales of order 10 Myr (e.g. [5,6]), compatible with the standard view of giant planet formation by dust coagulation, planetesimal formation, and core accretion of nebular gas, as indicated by the fossil record of the planets in our Solar System [7]. This rough outline of the planet formation process is certainly incomplete. For example, the core accretion model has trouble accounting for the formation of ice giant planets at the distances of Uranus and Neptune on timescales shorter than the disk dissipation time. An alternative model postulates that gas giant protoplanets form very rapidly (in just $\sim 10^3$ years) by disk instability, where the gas in a marginally gravitationally unstable disk forms clumps that then contract to planetary densities [8]. In addition, the discovery that extrasolar giant planets at <0.05 AU from their parent stars are common, together with their distributions in radius and eccentricity, indicates that giant planets likely migrate inward from formation zones

farther out in the disk (e.g. [9]). The dynamical evolution of these migrating giant planets depends sensitively on the physical properties of the disk, in particular the surface density structure and the gas dissipation time [10]. These dynamical mechanisms have important consequences for the formation and survival of terrestrial planets in the inner disk, which must arise from collisional accumulation of rocky planetesimals.

Spatially unresolved panchromatic observations of the spectral energy distributions of protoplanetary disks will continue to lead to new insights, but direct imaging is ultimately essential to form a complete picture, to verify theoretical constructs, and to break model degeneracies.

3. SKA Sensitivity and Imaging Feasibility

Dust emissivity drops steeply toward long wavelengths, and thermal emission from dust at the high angular resolution appropriate to the inner regions of protoplanetary disks is very weak by the standards of today. Remarkably, the SKA will be sufficiently sensitive to image dust emission with brightness of ~ 100 K at milliarcsecond resolution in very reasonable integration times.

For a geometrically thin disk, the flux dS from a dusty disk element filling solid angle $d\Omega$ is

$$dS = B_{\nu}(T)(1 - e^{-\tau_{\nu}}) \cos i \, d\Omega \quad (1)$$

where $B_{\nu}(T)$ is the Planck function, i is the inclination, and the optical depth τ_{ν} is given by

$$\tau_{\nu} = \Sigma \kappa_{\nu} / \cos i \quad (2)$$

where Σ is the surface density and κ_{ν} is the dust mass opacity. To make an estimate for the SKA, we assume an observing frequency of 22 GHz, a conservative fiducial value that represents a compromise between the rapid increase in flux with frequency, the increase with opacity with frequency, and the likely decrease in SKA sensitivity with frequency. The optimal choice of observing frequency will depend on details of the system performance and the distribution of collecting area with baseline length, and it is likely to be in the range of 22 to 34 GHz. With these

assumptions, the disk optical depth is

$$\tau_\nu = 0.31 \left(\frac{\nu}{22 \text{ GHz}} \right) \left(\frac{\Sigma}{100 \text{ g/cm}^2} \right) \left(\frac{\cos i}{\cos 45} \right)^{-1} \quad (3)$$

and, for low optical depth in the Rayleigh-Jeans regime

$$dS = 0.11 \mu\text{Jy} \left(\frac{T}{300 \text{ K}} \right) \left(\frac{\Sigma}{100 \text{ g/cm}^2} \right) \times \left(\frac{\nu}{22 \text{ GHz}} \right)^3 \left(\frac{\theta}{2 \text{ mas}} \right)^2 \quad (4)$$

where θ is the synthesized beam Gaussian FWHM size. At 22 GHz, an angular resolution of 2 milliarcseconds requires baseline lengths of ~ 1500 km. If the SKA reaches an rms sensitivity of $\sim 0.02 \mu\text{Jy}$ in 8 hours, as expected, then dust emission from the inner regions of disks where the brightness temperature exceeds 100 K and the optical depths approach unity will be detectable in hours, and it may be imaged with high signal-to-noise in a few tens of hours. Since brightness temperature sensitivity is proportional to synthesized beam area, a survey of many sources could be made at somewhat lower angular resolution to identify those of most interest for the highest resolution imaging in a small fraction of this time per source. Note that the typical 22 GHz flux integrated over an entire protoplanetary disk spanning a few arcseconds on the sky is of order $\sim 100 \mu\text{Jy}$.

For sources at ~ 150 pc, a flux level of $\sim 0.1 \mu\text{Jy}$ at 22 GHz corresponds to less than an Earth mass of an interstellar mixture of gas and dust filling a 2 milliarcsecond beam, using the mass opacity adopted here. Thus the SKA will be able to discern mass concentrations that could be the seeds of giant planets that will form via the gravitational instability mechanism, as well as the spiral density waves of modest contrast expected to be driven by otherwise invisible embedded giant protoplanets and lower mass protoplanets.

Observations at 22 to 34 GHz with the SKA will be also sensitive to small amounts of ionized gas in the star-disk system, if present. A plasma could contaminate the signal from dust emission, though any contamination can be estimated accurately via extrapolation of longer wavelength

data and/or recognized from its spatial distribution, which will be different from the dust that fills the disk. For example, some T-Tauri stars are known to have chromospheric activity, which will be clearly indicated by a high brightness signal localized to transient magnetic features comparable in extent to the star. It's conceivable that additional compact emission features like this may prove helpful for calibration purposes on the longest baselines.

4. Grain Growth Studies

One mysterious aspect of the planet building process is how sub-micron size interstellar dust grains overcome energetic obstacles that prevent sticking, grow to sizes large enough to decouple from the disk gas, interact gravitationally, and build up to planetesimal sizes. This is a critical first step in the development of both giant planet cores and rocky planets. Most models postulate a phase of collisional agglomeration mediated by mechanisms like Brownian motion and turbulence. Numerical simulations of dust evolution indicate a bimodal distribution of particle sizes develops as centimeter-size aggregates grow and settle to the mid-plane (e.g. [11]). The resulting dense layer becomes the reservoir for the formation of larger bodies. Figure 2 shows the particle size distributions as a function of height from one such calculation; note the large population of centimeter-sized grains in the mid-plane.

The wavelength dependence of the dust emissivity provides a diagnostic of particle size, and dust in many protoplanetary disks shows evidence for size evolution from a primordial interstellar distribution [12,13]. There is ample evidence that the spectral slope of dust emission from T-Tauri stars in the millimeter regime is significantly lower than in diffuse molecular clouds, where the power-law exponent of the dust emissivity $\beta = 2$. For example, the spectral slope of the TW Hya disk shows a shallow dependence of emissivity on frequency between 1.3 mm (230 GHz) and 7 mm (43 GHz), with $\beta \sim 0.7$ (and resolved images confirm that optical depth effects do not affect this determination). For compact spherical particles of size $<< \lambda$, $\beta = 2$, while for

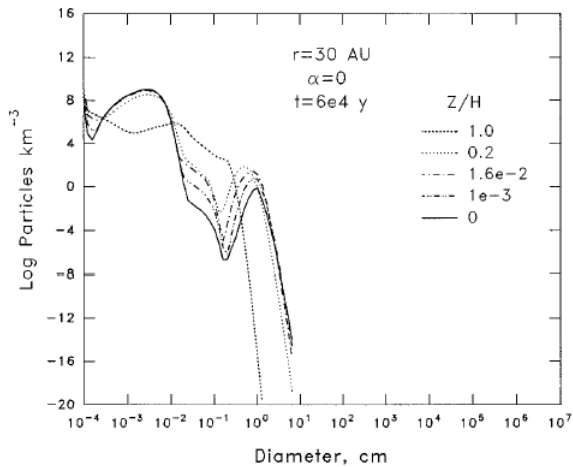


Figure 2. A numerical simulation of particle size evolution within a protoplanetary disk (from [11]). The small grains in the disk stick and settle to the mid-plane, which creates a layer of centimeter size particles. The plot shows the particle size distribution at different elevations, with the mid-plane that contains most of the mass indicated by a solid line.

particles of size $\gg \lambda$, $\beta = 0$. In realistic astrophysical mixtures, the value of β also depends on grain composition, structure, and topology, though the particle size generally dominates, especially for common silicates [14]. A substantial mass fraction of the dust grains in protoplanetary disks has apparently evolved and started to agglomerate. The low values of β derived from observations of TW Hya and a few other stars are robustly interpreted as evidence for particle growth to sizes of order a millimeter or more [2,15].

In general, observations are sensitive to particles with sizes of less than a few wavelengths, since the absorption cross section cannot depart significantly from the geometric cross section. The SKA, by observing dust emission at short centimeter wavelengths, can probe the presence of particles larger than a millimeter, a critical regime. Historically, inadequate sensitivity and spatial resolution have thwarted the goal of detecting these “pebbles”, since the opacity per unit mass decreases for larger particles and the resulting emission is weak. The SKA will allow for the first time multi-wavelength imaging that will localize regions within the disks with different spectral signatures and therefore different grain properties. The observed spatial variations in resolved images, together with dust models, will shed light on the roles of settling and turbulent entrainment in the grain growth process. Resolved observations at centimeter wavelengths will address the argument that grain growth to sizes of at least 1 cm are necessary before particles start settling to the mid-plane because smaller grains are stirred by turbulence [16].

5. Disk Structure: State-of-the-Art

While current observational capabilities are a far cry from the potential of the SKA, the results and their interpretation offer a glimpse at the possibilities for future observations of protoplanetary disks with higher angular resolution and sensitivity. The currently operating millimeter arrays routinely detect large numbers of nearby protoplanetary disks, and the ongoing upgrades to shorter wavelengths and longer baselines are

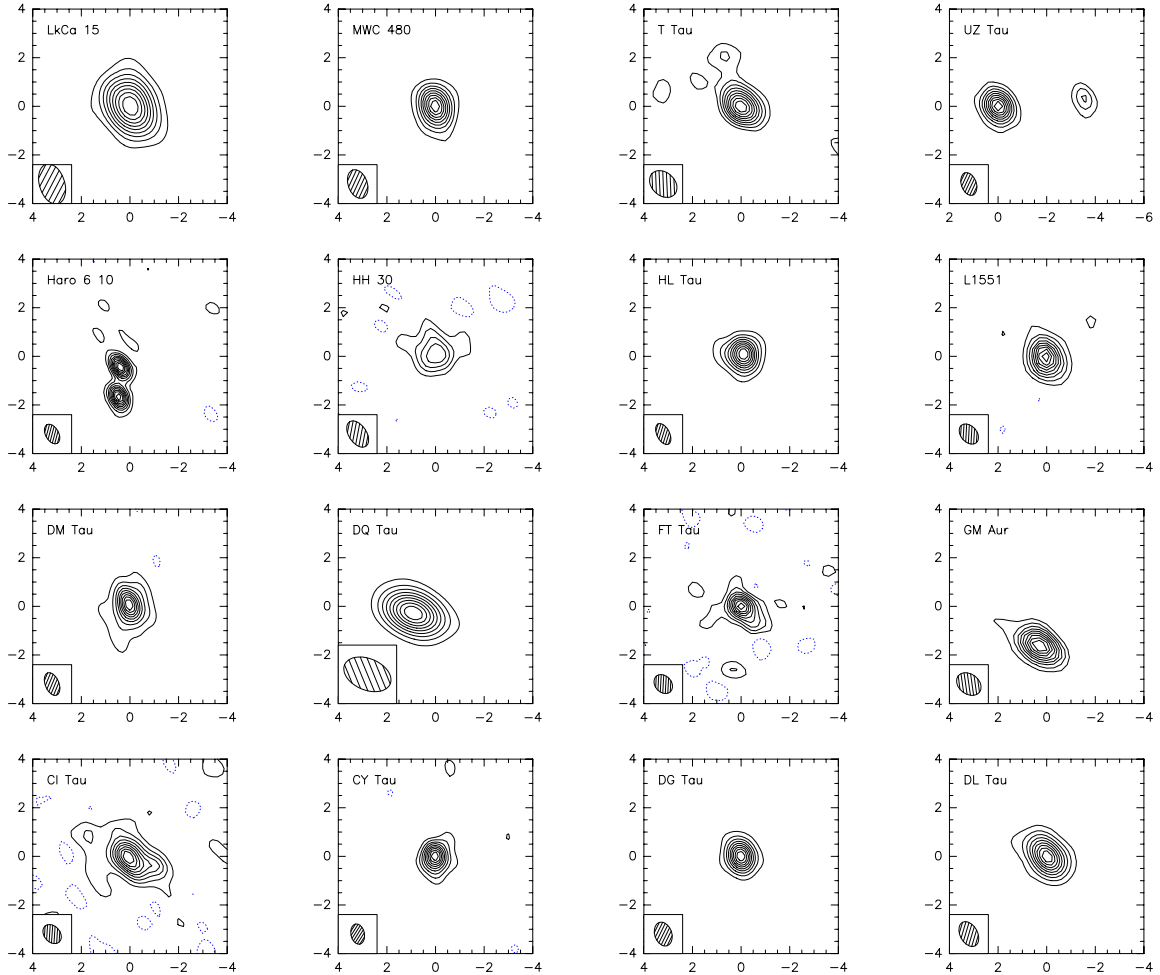


Figure 3. Survey of Taurus pre-main-sequence stars (single and multiple) from the IRAM Plateau de Bure Interferometer at 230 GHz with typical resolution $0.^{\prime\prime}5$, or 70 AU (from [20]). Contours are 10% of the peak. The optically thin dust brightness from the circumstellar disks falls steeply with radius in the outer disk, and it rapidly falls below the sensitivity threshold. Nonetheless, most of the disks are resolved, and these images provide useful limits on the disk size, orientation, and overall surface density structure. The inner disk regions of planet formation are not probed, primarily because of beam dilution. The SKA will push imaging of thermal dust emission in the high column density inner disks to sub-AU scales, at lower frequencies where dust opacity is low enough to penetrate through the full disk column.

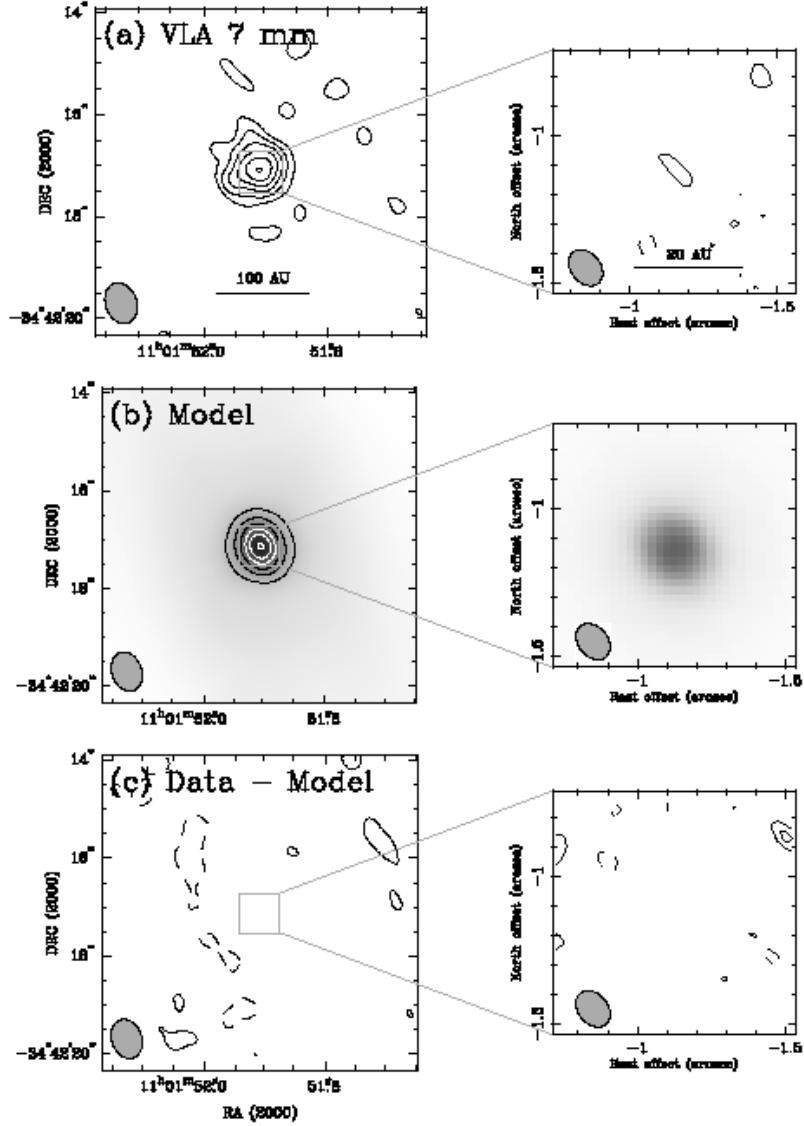


Figure 4. VLA 43 GHz images of TW Hya compared to the accretion disk model that fits the spectral energy distribution shown in Figure 1 (from [2]). (a) VLA 43 GHz images of TW Hya at two resolutions. (b) Simulated VLA images of the disk model brightness distribution with the same contours and beam sizes as in (a). The gray-scale shows extended emission, most of which remains undetectable with the available sensitivity. (c) Difference images obtained by subtracting visibilities derived from the model from the data.

just starting to provide spatially resolved information. With considerable effort, several interferometric imaging *surveys* of tens of T Tauri stars with $0''.5$ resolution have been completed, and a few observations have pushed the angular resolution frontier to $\sim 0''.1$.

5.1. Dust Emission Surveys

The first major survey of the disks around T-Tauri stars was performed with the IRAM Plateau de Bure interferometer at 110 GHz [17], with follow-up observations at 230 GHz [18]. This survey produced the very important first measurements of well-resolved sizes for a sizable subset of the observed sample. Figure 3 shows a set of high resolution 230 GHz images of sources in Taurus. Careful modeling of the observations implied disks around single stars with large outer radii, $R > 150$ AU, and rather shallow radial surface density profiles, $\Sigma \propto r^{-p}$, $p < 1.5$. These shallow surface density profiles imply that only a small fraction of the disk mass is located in the inner disk, a difference from the conventional assumptions of Solar Nebula models. The uniform nature of such surveys allows for investigation of correlations between the derived disk parameters and various evolutionary markers. An intriguing result from a similar survey using the Nobeyama Millimeter Array [19] is that the disk outer radius increases with decreasing H α luminosity, perhaps due to radial expansion with age, as expected in accretion disks by transfer of angular momentum.

5.2. The Angular Resolution Frontier

The highest resolution at millimeter wavelengths comes from the Very Large Array augmented by the link to the Pie Town VLBA antenna, attaining a resolution of 30 milliarcseconds at 43 GHz, albeit with limited brightness temperature sensitivity [21]. Figure 4 shows VLA images of TW Hya at 43 GHz at two different resolutions obtained with different visibility weighting schemes [22]. The lower resolution image in the left panel has a $\sim 0''.6$ (56 AU) beam that emphasizes the spatially extended low brightness emission. The region of detectable 43 GHz emission at this resolution is ~ 100 AU in diameter, and a fainter halo extends to larger distances. The

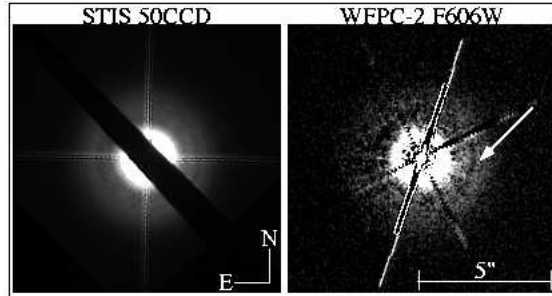


Figure 5. The TW Hya disk imaged in scattered light from the STIS and WFPC 2 instruments on the Hubble Space Telescope (from [23]). The inner disk regions are inaccessible at these wavelengths because of the bright central star.

image in the right panel has a $\sim 0''.1$ (5.6 AU) beam. Little detectable emission is visible from TW Hya at this scale. Only the orders of magnitude improvement in sensitivity and resolution from the SKA will allow imaging at substantially higher resolution.

A comparison of the thermal dust emission images of the TW Hya disk with scattered light images is illuminating. In the optical, the best angular resolution and image quality comes from the Hubble Space Telescope. Figure 5 shows the Hubble images of TW Hya from STIS (using coronography) and WFPC 2 (using PSF subtraction), both of which dramatically reveal the full extent of this nearly face-on disk in scattered light [23]. These images also emphasize the unavoidable problems of probing the inner regions of protoplanetary disks in scattered light, since the star dominates and must be blocked or removed to very high accuracy to extract the faint disk signal, a process that becomes exceedingly difficult in the immediate neighbourhood of the central star.

5.3. Physical Models

Physical models of disk structure and evolution are becoming more sophisticated as more physics is incorporated and better computational meth-

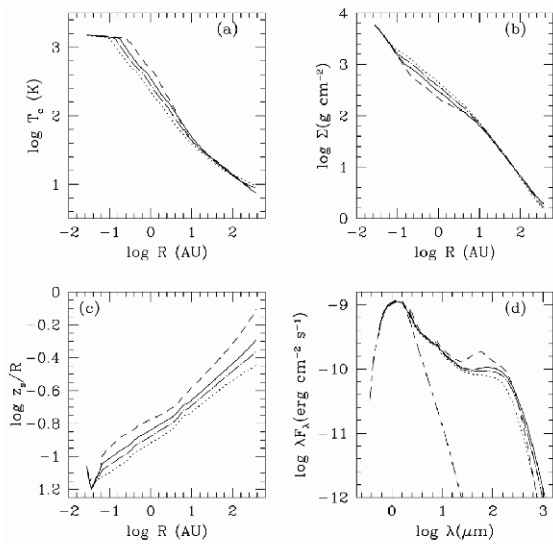


Figure 6. Results of a self-consistent accretion disk calculation for a typical T Tauri star (from [24]). The panels show the radial distribution of (a) mid-plane temperature, (b) mass surface density, (c) height of the irradiation surface divided by radius. Panel (d) shows the spectral energy distributions for a pole-on viewing geometry (the central star is indicated by the long-short dashed line). The four curves in each panel correspond to different assumptions about dust grains in the model, which start to depart significantly within the inner disk regions that can be imaged only by the SKA.

ods are implemented. Several groups have developed self-consistent treatments of disks around young stars in radiative and hydrostatic equilibrium, employing radiative transfer schemes with various degrees of complexity (e.g. [24,25]). An important trend is to interpret high angular resolution data in the context of these models. Figure 6 shows the results of one such calculation, the irradiated accretion disk model of D'Alessio et al. (2001) [24].

The basic features of the radial dependences that arise in this model are readily explained. For steady accretion, the surface density is given by

$\Sigma = \dot{M}/3\pi\nu$ away from the boundaries, where \dot{M} is the accretion rate, and $\nu = \alpha c_s H$ is the kinematic viscosity parameterized by a local velocity (the sound speed, c_s), scale length (the scale height, H) and a dimensionless parameter ($\alpha < 1$). The surface density may be expressed as $\Sigma \propto (r^{3/2} T_m)^{-1}$, where T_m is the local mid-plane temperature whose value is determined by the balance of heating by stellar irradiation and viscous processes, and cooling through radiative losses. For a disk with heating dominated by stellar irradiation, the flaring of the outer parts of the disk tends to drive the temperature distribution to $T_m \propto r^{-1/2}$, except in the innermost regions where the disk becomes optically thick to its own radiation, and $\Sigma \sim r^{-1}$.

The existing resolved images of the TW Hya disk at 43 GHz and at 345 GHz match this model very well [26]. The middle panel of Figure 4 shows the result of imaging the model brightness distribution at these two angular resolutions using the same visibility sampling as the VLA observations. The lower panel of Figure 4 shows the residual images obtained by subtracting the model visibilities from the VLA data and then imaging the difference with the standard algorithms; there are no significant residuals.

The increasing sophistication of the physical models is leading to progress on many fronts. For example, a consequence of the modest brightness of the TW Hya disk observed within 5 AU is that the surface density is unlikely to be very much higher in this region of the disk than expected from an r^{-1} extrapolation to smaller radii. A region of low viscosity and concomitant high surface density in the inner disk appears to be required by some mechanisms for accretion, planet formation, and also planet migration. For example, the layered accretion of Gammie (1996) [27] piles up accreting mass in a “dead zone” where the magneto-hydrodynamic instability does not operate very effectively. For TW Hya, there is no evidence for any such substantial mass reservoir at these small radii. Indeed, the existing data suggest a mass deficit, which may be related to a deficit of mid-infrared emission and a possible large central hole cleared out by a developing protoplanet (see §6). On the large scale, if the ac-

cretion disk model for TW Hya is valid, then the fact that the surface density normalization based on the mass accretion rate (estimated from ultraviolet excess) and viscosity parameter α (~ 0.01) agrees with the millimeter result provides indirect support for the adopted mass opacity law.

Figure 6 shows that the physical structure of the disks start to depart from general power law behaviors in the innermost regions, where the models become dependent on several parameters that are poorly constrained by existing observations. The differences among the four disk models shown in each panel of Figure 6 result from different assumptions about the grain size distribution. The inner regions that are affected will be accessible to the SKA, and these assumptions may be tested.

6. Planet Signatures: Disk Gaps

An important theoretical prediction is that planets in disks, once they achieve sufficient mass, will interact with the disk material and open wide radial gaps – large regions of low surface density – around their orbits [28]. The formation of gaps could be significant in limiting the growth of giant planets [29]. As noted in §2.3, the tidal interaction between a giant protoplanet and its disk can result in orbital migration (e.g. [30]), and this process affects the orbital distribution of giant planets (and perhaps also their survival if migration is not halted.) Because the gaps opened by the protoplanets are much larger than the protoplanets themselves, this gap imprinted on the disk may be the best observational signature of protoplanet formation.

6.1. Why Gaps?

The basic idea behind gap formation is that an orbiting protoplanet tidally interacts with its parent disk. Material exterior to the planet gains angular momentum from the planet and moves to larger radii, while material interior to the planet loses angular momentum and moves to smaller radii, creating a gap. Viscous processes tend to act against tidal forces and fill in the developing gap. Whether or not the tidal forces overcome the viscous processes depends on the mass ratio

q of the planet and the star, and the Reynolds number, $\mathcal{R} = \Omega r^2 / \nu$, where Ω is the angular frequency, r is the radius, and ν is the kinematic viscosity (often parameterized using the α prescription). If $q > \mathcal{R}^{-1}$, then a gap forms.

Figure 7 shows the result of a representative calculation where the disk surface density is perturbed and develops a gap [29]. In this hydrodynamic simulation, the mass ratio, q , is 10^{-3} , and trailing spiral density waves are excited near the inner and outer Lindblad resonances of the protoplanet. Shock dissipation of waves deposit angular momentum, and the disk material moves away from the protoplanet orbit. The gap width is $\sim 20\%$ of the orbital radius, or ~ 1 AU for a Jupiter at 5 AU. More sophisticated simulations are now being undertaken that include prescriptions for magnetohydrodynamical turbulence [31] and fully three dimension hydrodynamics [32], and the results are qualitatively very similar. For typical initial conditions, planets with masses as low as ~ 0.1 Jupiter mass open significant gaps, though lower mass planets launch spiral waves and produce potentially detectable large scale disturbances. Since the physical conditions of the inner disk are poorly constrained, and the sources of disk viscosity are even more poorly understood, such results will undoubtedly undergo revision. In principle, the properties of the protoplanets ultimately may be constrained in detail by measurements of the gap locations and widths, and the amount of residual material within the gaps.

6.2. Evolutionary Issues

The subsequent evolution of a disk with a gap induced by a protoplanet may include accretion of material inside the protoplanet orbit to produce an inner evacuated hole, if gas from the outer disk is prevented from accreting across the gap. The formation of Jupiter in our Solar System might have prevented the outer disk gas from reaching interior regions and allowed the inner disk gas to fully accrete, leaving behind solid planetesimals to form terrestrial planets. But if the planet were to lose angular momentum due to torques from a sufficiently massive outer disk, then the Jupiter would migrate inward and sweep away any interior rocky planets. Observations are needed to

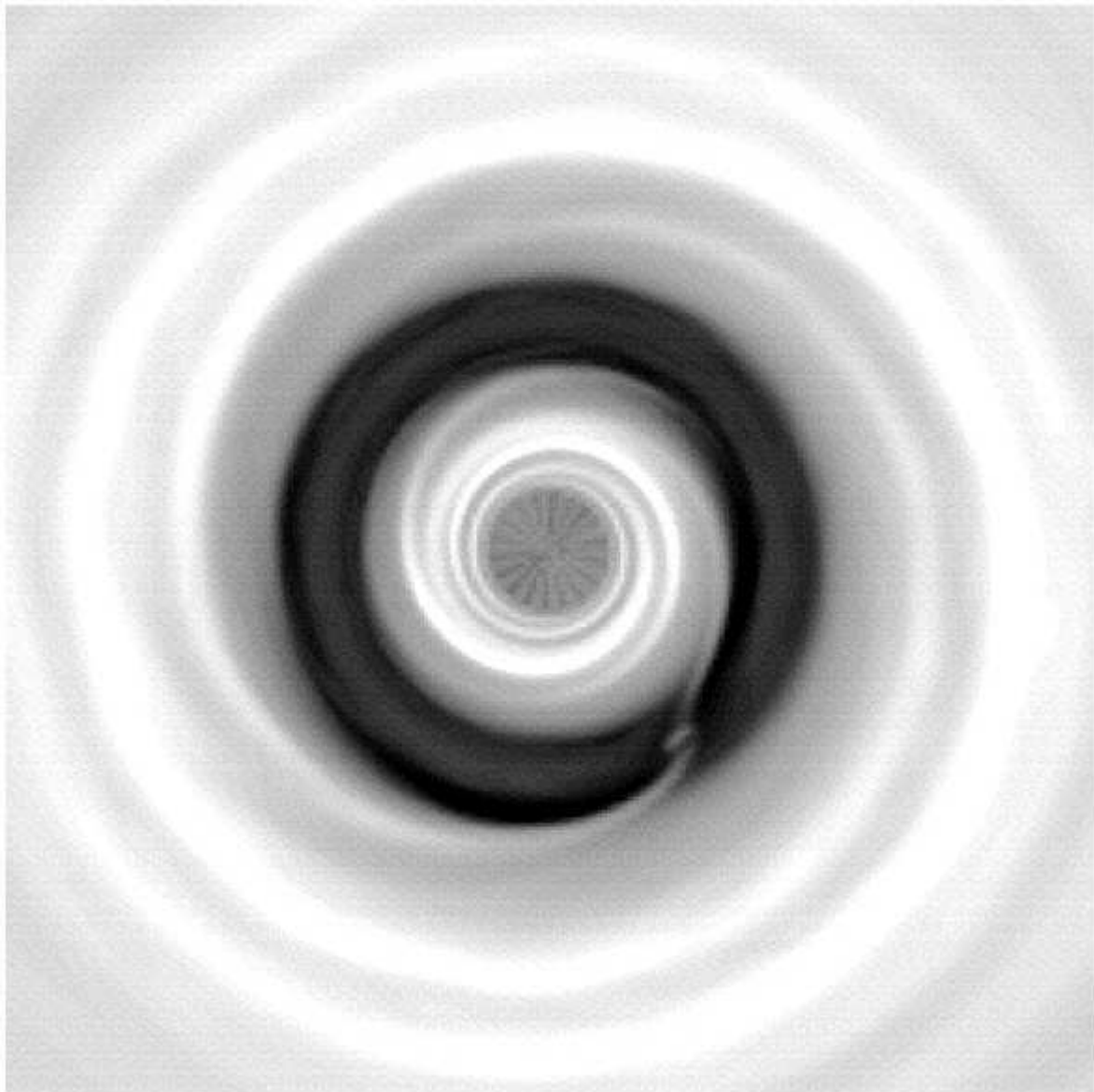


Figure 7. A numerical simulation of a Jupiter mass planet within a disk that opens up a gap in the disk through tidal interaction (from [29]). The dark region in this surface density plot is nearly devoid of disk material. The planet is located within the dark region, in a small accretion stream. While the planet itself is extremely difficult to detect at any wavelength, the wide gap provides a strong marker of its presence, and the gap structure might be used to constrain its properties.

inform the frequency of such disparate outcomes of the planet building process.

6.3. Observing Gaps

Disk gaps may manifest themselves in spectral energy distributions as the deficit of disk material over a limited range of radii results in less emission in a limited wavelength range. A gap close to the star might result in a deficit of mid-infrared emission, which is otherwise dominated by close-in material. Some T-Tauri stars, for example TW Hya, GM Aur, and CoKu Tau 4, have mid-infrared deficits that indicate the inner disks have been cleared out to radii of a few AU or more. Less dramatic perturbations in the disk structure, such as spiral waves generated by a low mass planet, will have more subtle effects on the spectral energy distribution, and it is likely they will be revealed only by direct imaging of surface density structure.

If the predicted gaps are present in the inner disk, SKA images of dust emission will show them. Such gaps, if they are not devoid of gas, may have spectral signatures at infrared wavelengths, for example emission in the CO fundamental lines at $4.7\ \mu\text{m}$, which should be detectable with large optical telescopes [33]. Such gaps may also slightly modify the visibilities obtained by interferometers operating at infrared wavelengths, though teasing out the influence of the gaps from other model parameters may be impossible [34]. The SKA will be unique in *directly imaging* the gaps, which will avoid any ambiguities in the interpretation of unresolved observations, or highly model dependent results.

It is worth noting that ALMA will not have sufficient angular resolution to probe structure in the habitable zone of the nearby disks. In its most extended antenna configuration, the angular resolution will be only 20 milliarcseconds at 345 GHz (3 AU at 150 pc). In an optimistic scenario, ALMA will be able to reveal the gap created by a Jupiter orbiting at 5 AU [34]. The high dust opacity at these high frequencies also will be problematic for investigating the inner disk. Observations of inner disk structure must be made in the optically thin regime at lower frequencies using the SKA.

7. Proper Motions

Observations of dust emission do not provide any kinematic information directly, but the orbital timescales are sufficiently short that *synoptic* studies can follow the proper motions of mass concentrations and structures within the disk. At a characteristic radius of 1 AU from a T-Tauri star of $\sim 1\ M_\odot$, the full orbital period is ~ 1 year. Thus a series of images of several disk systems with identifiable features could be made at intervals of approximately a month, thereby providing good coverage of one orbit or more. These short timescales will permit the tracking of secular changes in disk structure related to the presence of planetary mass bodies. A wide spectrum of resonant interactions are possible that may produce dynamical signatures such as spiral waves. In addition, proper motions of features monitored over time will allow for clear discrimination of faint disk structures from any sources of confusion that might be present in the extragalactic background.

8. Summary

The SKA will play a pivotal role in understanding terrestrial planet formation by imaging thermal dust emission from the inner regions of protoplanetary disks around nearby young stars. The observations will probe the dense disk material at size scales of 1 AU, commensurate with the orbit of the Earth around the Sun. SKA imaging will reveal structures produced by embedded protoplanets whose motions can be tracked over time in a rich and representative sample of currently forming Solar Systems. Future optical and infrared planet searches may reveal terrestrial planets that could harbor life, but it will be left to the SKA to tell us why they are there and why we are here.

D.J.W. acknowledges support from NASA Origins of Solar Systems Program grant NAG5-11777. Thanks to Sean Dougherty, Lewis Knee and others in the SKA Working Group on the Life Cycle of Stars for many valuable contributions.

REFERENCES

1. Beckwith, S.V.W. & Sargent, A.I. 1996, *Nature*, 383, 139
2. Calvet, N., D'Alessio, P., Hartmann, L., Wilner, D., Walsh, A., Sitko, M. 2002, *ApJ*, 568, 1008
3. Adams, F.C., Lada, C.J. & Shu, F.H. 1987, *ApJ*, 312, 788
4. Beckwith, S.V.W., Sargent, A.I., Chini, R. Gusten, R. 1990, *AJ*, 99, 924
5. Strom, K.M., Strom, S.E., Edwards, S., Cabrit, S., Skrutskie, M.F. 1989, *AJ*, 97, 1451
6. Haisch, K.E., Lada, C.J., Lada, E.A. 2001, *ApJ*, 553, 153
7. Wuchterl, G., Guillot, T., Lissauer, J.J. in *Protostars and Planets IV*, eds. V. Mannings, A. Boss and S. Russell, p. 1081
8. Boss, A.P. 1997, *Science*, 276, 1836
9. Lin, D.N.C., Bodenheimer, P., Richardson, D.C. 1996, *Nature*, 380, 606
10. Goldreich, P. & Sari, R. 2003, *ApJ*, 585, 1024
11. Weidenschilling, S.J. 1997, *Icarus*, 127, 290
12. Beckwith, S.V.W. & Sargent, A.I. 1991, *ApJ*, 381, 250
13. Beckwith, S.V.W., Henning, T., Nakagawa, Y. 2000, *Protostars and Planets IV*, eds. V. Mannings, A. Boss and S. Russell, p. 533
14. Pollack, J.B., Hollenbach, D., Beckwith, S., Simonelli, D.P., Roush, T. 1994, *ApJ*, 421, 615
15. Natta, A., Testi, L., Neri, R., Shepherd, D.S., Wilner, D.J. 2004, *A&A*, 416, 179
16. Weidenschilling, S.J. 2000, in "From Dust to Terrestrial Planets", proceedings of an ISSI Workshop, eds. W. Benz, R. Kallenbach, and G. W. Lugmair, p. 295
17. Dutrey, A., Guilloteau, S., Duvert, G. Prato, L., Simon, M., Schuster, K., Menard, F. 1996, *A&A*, 309, 493
18. . Guilloteau, S., Dutrey, A., Gueth, F. 1997, proceedings of IAU Symposium No. 182, eds. Bo Reipurth and Claude Bertout, p. 365
19. Kitamura, Y., Momose, M., Yokogawa, S., Kawabe, R., Tamura, M. Ida, S. 2002, *ApJ*, 581, 357
20. Dutrey, A. 2001, proceedings of IAU Symposium No. 200, eds. Hans Zinnecker and Robert D. Mathieu, p. 219
21. Wilner, D.J. 2002, in "The Origins of Stars and Planets: The VLT View", Springer-Verlag series of ESO Astrophysics Symposia, eds. J. Alves and M.J. McCaughrean, p. 311
22. Wilner, D.J., Ho, P.T.P., Kastner, J.H., Rodriguez, L.F. 2000, *ApJ*, 534, L101
23. Schneider, G., Hines, D.C., Silverstone, M.D., Weinberger, A.J., Becklin, E.E., Smith, B.A. 2001, *ASP Conference Series* Vol. 245, eds. Ted von Hippel, Chris Simpson, and Nadine Manset, p. 121
24. D'Alessio, P., Calvet, N., Hartmann, L. 2001, *ApJ*, 553, 321
25. Dullemond, C.P., Natta, A. 2003, *A&A*, 408, 161
26. Qi, C., Ho, P.T.P., Wilner, D.J., Takakuwa, S., Hirano, Ohashi, N., Bourke, T.L., Zhang, Q., Blake, G.A., Hogerheijde, M., Saito, M., Choi, M., Yang, J. 2004, *ApJ*, in press
27. Gammie, C. 1996, *ApJ*, 457, 355
28. Lin, D.N.C. & Papaloizou, J.C.B. 1979, *MNRAS*, 186, 799
29. Bryden, G., Chen, X., Lin, D.N.C., Nelson, R.P., Papaloizou, J.C.B. 1999, *ApJ*, 514, 344
30. Lin, D.N.C. & Papaloizou, J.C.B. 1986, *ApJ*, 307, 395
31. Papaloizou, J.C.B., Nelson, R.P., Snellgrove, M.D. 2004, *MNRAS*, 350, 829
32. Bate, M.R., Lubow, S.H., Ogilvie, G.I., Miller, K.A. 2003, *MNRAS*, 341, 213
33. Najita, J., Carr, J.S., Mathieu, R.D. 2003, *ApJ*, 589, 931
34. Wolf, S., Gueth, F., Henning, T., Kley, W. 2002, *ApJ*, 566, L97